MOLECULAR AND CELLULAR BIOLOGY, Apr. 1997, p. 2066–2075 Vol. 17, No. 4
0270-7306/97/$04.00+0

Control of NFATx1 Nuclear Translocation by a Calcineurin-Regulated Inhibitory Domain

ESTEBAN S. MASUDA,[1] JIE LIU,[2] RYU IMAMURA,[1] SHIN-ICHIRO IMAI,[3] KEN-ICHI ARAI,[2] AND NAOKO ARAI[1]*

Department of Cell Signaling, DNAX Research Institute of Molecular and Cellular Biology, Palo Alto, California 94304,[1] and Department of Molecular and Developmental Biology, The Institute of Medical Science, University of Tokyo, Tokyo 108,[2] and Department of Microbiology, Keio University School of Medicine, Shinjuku-ku, Tokyo 160,[3] Japan

Received 20 September 1996/Returned for modification 7 November 1996/Accepted 7 January 1997

The nuclear factor of activated T cells (NFAT) regulates cytokine gene expression in T cells through *cis*-acting elements located in the promoters of several cytokine genes. NFATx1, which is preferentially expressed in the thymus and peripheral blood leukocytes, is one of four members of the NFAT family of transcription factors. We have performed domain analysis of NFATx1 by examining the effects of deletion mutations. We found that NFATx1 DNA binding activity and interaction with AP-1 polypeptides were dependent on its central Rel similarity region and that transcriptional activation was reduced by deletions of either its N-terminal domain or its C-terminal domain, suggesting the presence of intrinsic transcriptional activation motifs in both regions. We also identified a potent inhibitory sequence within its N-terminal domain. We show that the inactivation of the inhibition was dependent on the activity of calcineurin, a calcium-calmodulin-dependent phosphatase. We also show that calcineurin associated with the N-terminal domain of NFATx1 at multiple docking sites and caused a reduction of size, indicative of dephosphorylation, in NFATx1. We have mapped the inhibitory activity to less than 60 residues, containing motifs that are conserved in all NFAT proteins. Finally, we demonstrate that deletion in NFATx1 of the mapped 60 residues leads to its nuclear translocation independent of calcium signaling. Our results support the model proposing that the N-terminal domain confers calcium-signaling dependence on NFATx1 transactivation activity by regulating its intracellular localization through a protein module that associates with calcineurin and is a target of its phosphatase activity.

T cells become activated when they recognize peptides derived from foreign antigens in the context of antigen-presenting cells. Activated T cells then produce and secrete a plethora of cytokines, which are largely responsible for initiating and coordinating effective immune responses (1, 23, 25). The induction of cytokine gene expression and other downstream signaling events that occur during T-cell activation involve at least two distinct signaling pathways, since the combined action of calcium ionophores and phorbol esters can mimic these responses (6, 28). The calcium-dependent pathway is of particular interest because it is this pathway that is blocked by the action of the immunosuppressive drugs cyclosporin A (CsA) and FK506 (6). These drugs combine with immunophilins and prevent cytokine gene expression by inhibiting the phosphatase activity of calmodulin-dependent calcineurin (6).

The nuclear factor of activated T cells (NFAT) regulates induction of cytokine gene expression in T cells through *cis*-acting elements located in the promoters of several cytokine genes (6, 20, 27). NFAT is a multimeric complex whose components clarify, in part, the dual signaling requirements for induction of the interleukin-2 (IL-2) gene and other cytokine genes (6, 13). Transcription dependent on the distal NFAT-binding site from the IL-2 promoter, for example, requires the action of both phorbol myristate acetate (PMA) and calcium ionophore. The PMA requirement is primarily for the induction of the AP-1 heterodimers, and the calcium mobilization requirement is to activate preexisting cytoplasmic NFAT proteins (6, 27).

To date, four members of the NFAT family of transcription factors have been reported: NFAT1/NFATp, NFATc, NFAT3, and NFATx/NFAT4/NFATc3 (9, 10, 21, 22, 24). NFAT proteins are characterized by a highly homologous DNA-binding domain, which is weakly related to the DNA-binding domains of Rel family proteins (10, 21, 24). The high degree of similarity is manifested by the fact that all members are capable of binding and transactivating through the same IL-2 NFAT-binding site (10, 21, 22, 24). Another feature of NFAT proteins, perhaps even more distinctive, is a unique domain with moderate homology in their N termini preceding their DNA-binding domains. This domain contains several conserved motifs (9, 10, 16, 21), most of which are collectively encompassed by a ~300-residue region termed the NFAT homology region (NHR) (16). The C-terminal domains of NFAT proteins exhibit little homology.

The mechanism for calcium-dependent activation of NFAT proteins is under investigation. Recent work on NFAT1 regulation has shown that as calcium is mobilized, calcineurin is activated and binds NFAT1 (15, 37). Calcineurin then dephosphorylates NFAT1 (30, 32), resulting in its nuclear translocation (30, 32) and activation of its DNA binding activity (26).

Here we report a domain analysis of NFATx1, a splice variant of NFATx that is predominantly expressed in the thymus (21). We show the domains in NFATx1 involved in its DNA

* Corresponding author. Mailing address: Department of Cell Signaling, DNAX Research Institute of Molecular and Cellular Biology, 901 California Ave., Palo Alto, CA 94304. Phone: (415) 496-1260. Fax: (415) 496-1200. E-mail: arai@dnax.org.

binding activity, AP-1 interaction, and transcriptional activation. We also report the characterization of a potent inhibitory region in the N terminus of NFATx1 that is regulated by the serine/threonine calcineurin phosphatase.

MATERIALS AND METHODS

Cells. Jurkat (clone E6-1) cells and 293T (293tsA1609neo) cells, a 293 subline stably transfected with the simian virus 40 T antigen (7), were obtained from the American Type Culture Collection, Rockville, Md. Cells were grown at 37°C in an atmosphere containing 5% CO_2. 293T and COS-7 cells were grown in Dulbecco's modified Eagle medium, and Jurkat T cells were grown in RPMI 1640 medium, both supplemented with 10% heat-inactivated fetal calf serum, 4 mM L-glutamine, 100 U of penicillin per ml, and 100 mg of streptomycin per ml.

Plasmids. pME-NFATx (hereafter referred to as pME-NFATx1) and pME-NFATc are expression plasmids for NFATx1 and NFATc cDNAs under the control of the SRα promoter in vector pME18S and have been described previously (21). Plasmids containing deletions in NFATx1 were constructed from pME-NFATx1 by using standard recombinant DNA techniques (2). DNA fragments were deleted by using suitable restriction enzymes; when necessary, digested ends were filled in with Klenow fragment to ensure in-frame constructions upon ligation and transformation. At least two independent clones for each construct were selected, characterized, and used for transfection experiments. Junction nucleotide sequences in constructs were verified by DNA sequencing. pME-XΔC contains a deletion that includes the sequences encoding the carboxy terminus and 308 bp of 3′ untranslated sequence. pME-XΔRC and pME-XΔNC also lack the same 308 bp of 3′ untranslated sequence in addition to sequences indicated in Fig. 2A. pME-XΔGT was constructed by replacing a 493-bp fragment, excised with *Xba*I and *Bsa*AI from pME-NFATx1, with a 325-bp fragment obtained from a PCR product that had been digested with *Xba*I and *Bsa*AI. The PCR was performed using *Pfu* DNA polymerase (Stratagene, La Jolla, Calif.) with pME-NFATx1 as the template DNA and the following oligonucleotides as primers: 5′-GCTCTAGAACCCTTGGATCCCCTCTGACTTCT-3′ and 5′-AG CATTGAGCCACGTATCTTCTG-3′. pNFAT72Luc was obtained from Lisako Tsuruta (University of Tokyo, Tokyo, Japan) and contains the reporter luciferase gene under the control of three copies of the murine distal NFAT site (−290 to −261) (11). pCMV-SEAP (Tropix, Bedford, Mass.) is an expression vector of secreted alkaline phosphatase under the control of the cytomegalovirus promoter/enhancer. pBJ5-CNA and pBJ5-CNB, kindly provided by N. A. Clipstone and G. Crabtree (Stanford University, Stanford, Calif.), contain murine cDNAs for the Aα1 and B subunits, respectively, under the control of the SRα promoter (5).

Transfection and luciferase assays. Jurkat T cells were transiently transfected by the DEAE-dextran method with minimal modifications (2). Briefly, 5×10^6 cells were rinsed with 1× STBS buffer (25 mM Tris-Cl [pH 7.4], 137 mM NaCl, 5 mM KCl, 0.6 mM Na_2HPO_4, 0.7 mM $CaCl_2$, 0.5 mM $MgCl_2$). The cells were then resuspended in 750 μl of DEAE-dextran (500 μg/ml) in 1× STBS containing plasmid DNA (13 to 21 μg) and left at room temperature for 25 min. Next, 10 ml of 1× STBS buffer was added to dilute the DEAE-dextran solution, and cells were collected and resuspended in fully complemented culture medium. After approximately 40 h of incubation at 37°C, cells were stimulated for 8 h and supernatants and cell pellets were collected for subsequent enzymatic assays. In all transfections, pCMV-SEAP (2.5 μg) was included to monitor for transfection efficiency. Secreted alkaline phosphatase activity in supernatants of PMA-stimulated cells was measured in duplicate by a luminometer, using the Phospha-light assay system (Tropix). Luciferase in cell lysates was measured in duplicate by a luminometer, using a luciferase assay system (Promega, Madison, Wis.). Protein concentration was measured by using bicinchoninic acid (Pierce, Rockford, Ill.) as indicated by the supplier.

COS-7 cell transfection, Western blotting, and DNA binding. COS-7 cell transfections by the DEAE-dextran method and cytosolic extract preparations were carried out as described previously (21, 36). Cytosolic extracts were analyzed by sodium dodecyl sulfate (SDS)-polyacrylamide gel electrophoresis (PAGE) (4 to 12% gels) followed by Western blotting using an antiserum raised against the peptide GAHDELDFKLVFGEDGA (amino acids 7 to 23 of NFATx). The bands were visualized by enhanced chemiluminescence (Amersham, Arlington Heights, Ill.). DNA binding activity in the cytosolic extracts was examined by electrophoretic mobility shift assay (EMSA), using partially purified AP-1 from Jurkat cells as described previously (21).

Metabolic labeling of cells and immunoprecipitation. 293T cells were transiently transfected by the calcium phosphate method (2). Transfections were done in 100-mm-diameter dishes, using a maximum of 30 μg of total plasmid DNA in DNA-HEPES-buffered saline solution. Approximately 12 h later, the media was exchanged with fresh culture medium. Forty hours posttransfection, the cells were metabolically labeled with 500 μCi of Pro-mix (Amersham), an amino acid mixture containing [^{35}S]methionine and [^{35}S]cysteine, per 100-mm-diameter dish in methionine-free Dulbecco's modified Eagle medium for 4 h. Cells were lysed on ice for 30 min in lysis buffer (150 mM NaCl, 50 mM HEPES [pH 7.0], 10 μM $CaCl_2$, 0.25% Nonidet P-40, 10 μg of leupeptin per ml, 10 μg of aprotinin per ml, 10 μg of Pefabloc per ml, 1 mM sodium orthovanadate, 10 mM NaF, 1 mM sodium pyrophosphate). Immunoprecipitations were performed as described by Harlow et al. (8) and resolved on SDS–8 to 16% polyacrylamide gels. For immunoprecipitations, we used the rabbit antiserum (α-DS) raised against a bacterially produced recombinant peptide (residues 387 to 728) of human NFATx (14) or a rabbit antiserum raised against murine calcineurin B (CNB) (Affinity Bioreagents, Golden, Colo.).

Immunofluorescence staining. NFATx1 and XΔGT were visualized by immunofluorescence staining as reported by Liu et al. (14). Transfected COS-7 cells were either nonstimulated or stimulated with A23187 (0.5 μM) for 30 min, and the cells were fixed with 3.7% formaldehyde at room temperature. NFATx1 and XΔGT were stained with affinity-purified polyclonal antibody α-DS. The secondary antibody was fluorescein isothiocyanate-labeled goat anti-rabbit immunoglobulin G (Zymed, South San Francisco, Calif.).

RESULTS

Construction of NFATx1 deletion mutants. Based on degrees of similarity, NFAT proteins were divided into three main domains (Fig. 1A). The first, the N-terminal domain, comprises approximately 400 amino acids exhibiting modest similarity (23 to 35% identity) with patches of homology that represent nine conserved motifs (Fig. 1B) (9, 10, 21). The sequence encompassing the nine motifs has been referred to as the NHR (16) and includes three copies of the conserved SP box motif, SPXXSPXXSPXXXXX(D,E)(D,E) (21). The second, central domain, of about 300 residues, exhibits the highest similarity (66 to 73% identity) within NFAT sequences. This domain, referred to as the Rel similarity domain (RSD), is weakly similar to the DNA-binding domains of the Rel family of transcription factors (10, 12, 21, 24). The third, the C-terminal domain, of 250 to 350 residues, exhibits little similarity within NFAT proteins, except for a 15-amino-acid sequence that is present in at least one splice variant for each NFAT protein (11).

In view of their clear demarcations, we assumed that each domain constituted structurally independent folds and decided to investigate their function by constructing a series of expression plasmids of NFATx1 lacking one or two domains (Fig. 2A). All constructs derived from pME-NFATx1 (21), thus ensuring the use of the same transcriptional and translational regulatory sequences. Expression of the deleted constructs was confirmed by Western blot analysis. A blot of lysates of COS-7 cells transfected with the different plasmids was probed with a rabbit antiserum raised against a 17-amino-acid peptide (GA HDELDFKLVFGEDGA) present in the amino terminus of NFATx1 (Fig. 2B). A unique band for each construct was detected in each lane. In some lanes, additional bands of higher mobility were observed (Fig. 2B). These bands were not reproducible and were probably degradation products of the corresponding lower-mobility bands. The bands appearing in lysates from mock-transfected cells were nonspecific bands detected by the antisera.

NFATx1 DNA binding activity is dependent on the RSD. We then tested the different mutant constructs for DNA binding to the distal NFAT-binding site of the human IL-2 promoter (Fig. 2C). We previously showed that NFATx1 binding to the human NFAT-binding site required the presence of AP-1 (21). Thus, EMSAs using cytosolic extracts of COS-transfected cells were carried out in the presence of exogenously added AP-1. For comparison, we also included EMSAs with cytosolic extracts from cells that were transfected with the empty vector pME18S (mock) or with an expression plasmid of NFATc, an NFAT member which lacks most of the carboxy-terminus domain (24). The results indicate that, as for NFAT1 (12, 22), the RSD of NFATx1 contained the sequences responsible for DNA binding and AP-1 interaction. The smallest mutant able to bind the NFAT binding site was XΔNC, which contained an intact RSD (Fig. 2C, lane 8). Conversely, XΔRC and XΔNR, which lacked the RSD, were unable to bind DNA (Fig. 2C, lanes 7 and 9).

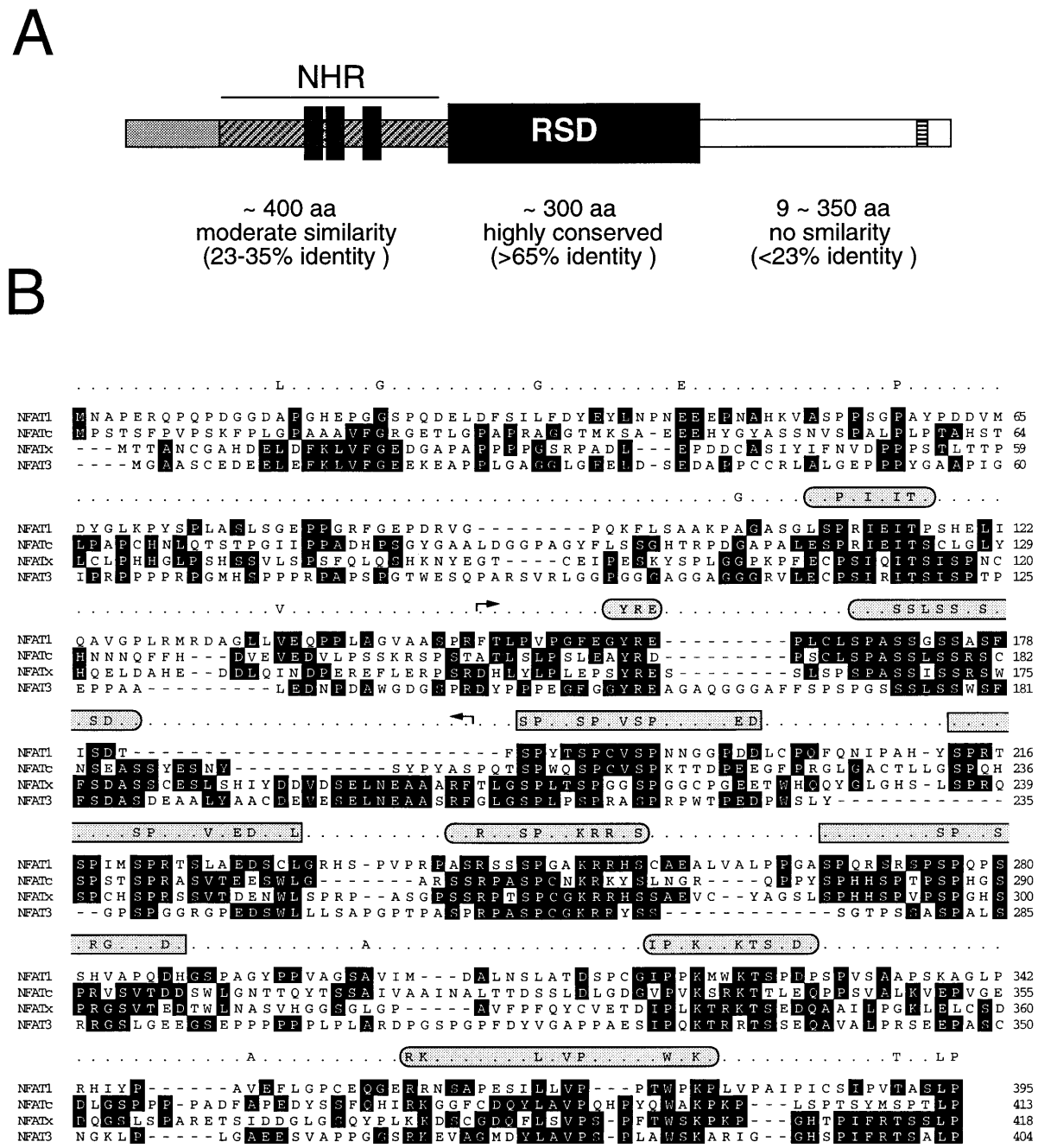

FIG. 1. (A) Schematic representation of a prototype NFAT protein. The RSD is represented by a solid black background and is labeled in white. The N-terminal domain is shown in gray and contains the ~300-residue NHR (hatched box). The three SP boxes are represented by small rectangles. The C-terminal domain (white box) exhibits no significant similarity, except for a 15-residue motif (small box with horizontal lines), which is present in at least one splice variant of each NFAT (11). aa, amino acids. (B) Alignment of amino acid sequences in N-terminal domains of human members of the NFAT protein family. Sequences for NFAT1 (16), NFATc (24), NFATx (10, 21), and NFAT3 (10) were aligned by using the Lasergene Megalign program (DNAstar, Madison, Wis.), with additional adjustments. Residues are numbered on the right and end at sequences corresponding to the start of their RSDs. Consensus residues, shown above the alignment, are a 100% match for the residue group. Residue groupings were as follows: DE; HKR; AGILV; NQ; FWY; ST; P; CM. Residues that match the consensus are shaded (with solid black). The consensus residues for the nine conserved motifs are shaded (SP box motifs, rectangles; others, ovals). Arrows demarcate the positions of residues deleted in XΔGT.

Effects of NFATx1 and deletion mutants on transcription driven by NFAT sites in Jurkat cells. We next checked the effects of NFATx1 and its deletions on transactivation activity elicited through NFAT-binding sites in Jurkat cells (Fig. 3). Either vector pME18S or the various NFATx1 expression plasmids were transfected along with reporter plasmid pNFAT72Luc, which contains the luciferase gene under the control of three copies of the murine IL-2 distal NFAT site. Consistent with previous reports (31), the luciferase activity of mock-transfected cells representing endogenous NFAT activity was dependent on stimulation with both phorbol ester (PMA) and calcium ionophore (A23187). Likewise, this NFAT activity was completely blocked by the action of CsA (Fig. 3A). Overexpression of NFATx1 increased luciferase activity by about 15-

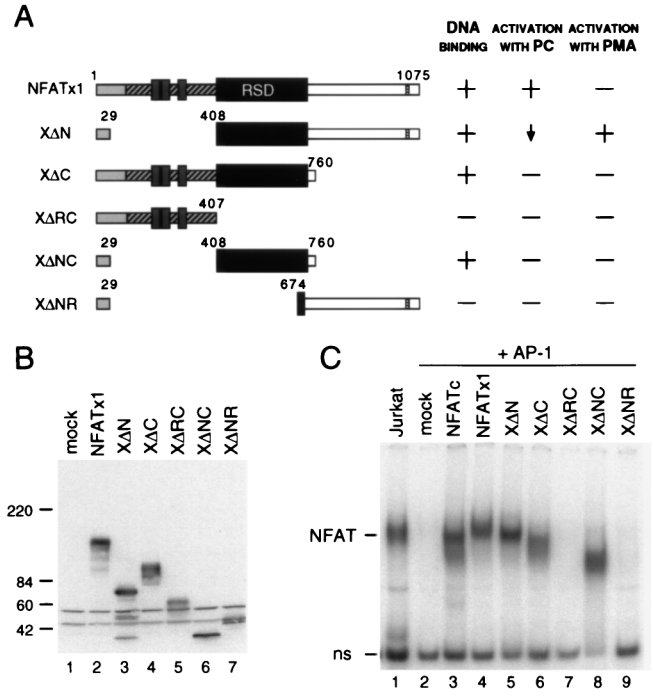

FIG. 2. Summary of NFATx1 deletion mutants. (A) Schematic diagrams of in-frame deletions of NFATx1 domains are shown, with numbers indicating the position of the residues remaining in the deletions. Activation with PMA or PC indicates transcriptional activation elicited by the construct after phorbol ester (PMA) stimulation or a combination of PMA and calcium ionophore (PC), respectively, as shown in Fig. 3. (B) NFATx1 and its deletions were detected by Western blot analysis of cytosolic extracts from transfected COS-7 cells with antisera raised against a 17-amino-acid peptide from the N terminus of NFATx1. Size markers are shown in kilodaltons on the left. Mock refers to COS-7 cells transfected with vector pME18S. (C) DNA binding to the distal NFAT-binding site of the human IL-2 promoter by the various NFATx1 deletion mutants. EMSAs were performed with cytosolic extracts from panel B. AP-1 was added exogenously to reconstitute DNA binding (21). Mock is pME18S vector alone. NFATc and Jurkat nuclear extracts were added as positive controls. Unbound probe is not shown. ns, nonspecific binding.

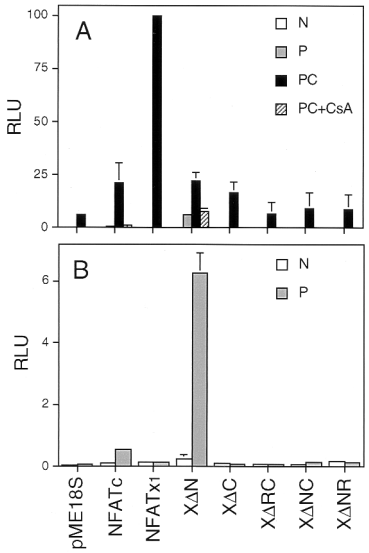

FIG. 3. Effects of NFATx1 and deletion mutants on transcription dependent on NFAT-binding sites. (A) Jurkat cells were transfected with 8 μg of pME18S, pME-NFATc, pME-NFATx1, or the indicated NFATx1 deletion construct along with pNFAT72Luc (3 μg) and pCMV-SEAP (2.5 μg). Thirty-six hours later, cells were stimulated for 8 h with PMA (50 ng/ml) (P), PMA and calcium ionophore A23187 (1.0 μM) (PC), or PMA and calcium ionophore plus CsA (1 μg/ml) (PC+CsA). N, nonstimulated cells. Luciferase activity values, given in relative luciferase units (RLU), were normalized to protein amounts in the lysates and to transfection efficiency. Transfection efficiency was monitored using pCMV-SEAP. The data are averages of three independent sets of experiments, where the values for NFATx1-transfected cells were set to 100 RLU. (B) Same as in panel A but showing values for nonstimulated cells and PMA-only-stimulated cells.

fold over endogenous activity; again, this activity was completely dependent on both PMA and A23187 stimulation and was sensitive to CsA action. This dependency is analogous to NFAT1 activity (16) but contrary to what has been reported for NFATc, which appeared to bypass the calcium signaling requirement (24). In our hands, however, addition of human NFATc led to a modest luciferase activity when activated with PMA alone (Fig. 3).

Deletion of any domain reduced the PMA-A23187-induced transactivation activity of NFATx1 (Fig. 3A), indicating the presence of sequences which are needed for full transactivation activity in both N-terminal and C-terminal domains. The decrease in transactivation activity could be caused by deletion of intrinsic transactivation domains or by structural defects affecting transcriptional activation, directly or indirectly. Evidently, XΔRC and XΔNR, by virtue of their inability to bind NFAT sites, were unable to activate transcription (Fig. 3A).

Interestingly, contrary to what was found for full-length NFATx1, transfection of pME-XΔN led to substantial luciferase activity when cells were stimulated with PMA only (Fig. 3B). This PMA-induced activity was equivalent to endogenous NFAT activity when cells were stimulated with the combination PMA-A23187. Moreover, this XΔN-directed activity was insensitive to the action of CsA (Fig. 3A). These results indicate that NFATx1 contains in its amino terminus an inhibitory sequence that is regulated by a calcium-calcineurin-dependent pathway.

Despite being substantial, the PMA-only activity elicited by XΔN corresponded to about a third of that activity stimulated with PMA-A23187 (Fig. 3A). This effect suggests that calcium mobilization affects additional pathways besides the inactivation of the inhibitory sequence. If this is the case, the pathways appear to be mediated by calcineurin as well, since addition of CsA inhibited the extra activity (Fig. 3A). Alternatively, it is possible that the inhibitory activity had only been partially deleted and that further deletions would lead to an activity completely independent of calcium signaling.

Finally, it should be noted that the PMA-only transactivation activity of XΔN was dependent on the C-terminal domain, since a deletion of this domain abolished all the activity (compare XΔN with XΔNC in Fig. 3B). This results reinforces the idea that the C-terminal domain contains an intrinsic transactivation domain.

Mobility shift of NFATx1 in SDS-PAGE is associated with the N-terminal domain. A peculiar feature of NFATx1 was observed in the Western blot in Fig. 2B. NFATx1 when expressed in COS-7 cells ran in SDS-PAGE at a mobility that was lower than expected from its deduced molecular mass (Fig. 2B; Table 1). NFATx1 had an apparent molecular mass of 137 kDa, which is about 20 kDa higher than its deduced molecular mass. The same discrepancy was observed for NFATx1 when expressed in 293T cells or Jurkat cells (19). This property is not unique to NFATx1, as it has been observed with NFAT1 and NFATc proteins (24, 30, 32). In these cases, it has been postulated that the size shift is due to phosphorylation events (30, 32).

Interestingly, the size discrepancy was not observed for

TABLE 1. Mobility shift of NFATx1 in SDS-PAGE is dependent on its N-terminal domain

Construct	Molecular mass (kDa)		
	Deduced	Apparent[a]	Discrepancy
NFATx1	116	137	21
XΔN	75	75	0
XΔC	83	99	16
XΔRC	44	63	19
XΔNC	42	42	0
XΔNR	45	48	3

[a] Results are representative of three different experiments. Similar values were obtained for COS-7, 293T, and Jurkat cells.

XΔN, XΔNC, or XΔNR, which lacked the N-terminal domain, while it remained for XΔC and XΔRC, which contained intact N-terminal domains (Fig. 2B; Table 1). Thus, these results demonstrate that sequences within the N-terminal domain were responsible for the mobility shift of NFATx1 in SDS-PAGE and were likely sites of phosphorylation.

The N-terminal domain of NFATx1 interacts with calcineurin. Recently, direct interactions between calcineurin and NFAT1 have been reported (15, 37). In view of the fact that the inhibitory region was regulated by calcineurin and that NFAT proteins had some similarities, we tested whether NFATx1 could also associate with calcineurin (Fig. 4). To determine the interaction, we cotransfected 293T cells with expression plasmids of NFATx1 along with expression plasmids of calcineurin A (CNA) and CNB or empty vector. The transfected cells were then metabolically labeled with [^{35}S]methionine and [^{35}S]cysteine, and their whole-cell lysates containing 10 μM $CaCl_2$ were used for immunoprecipitation experiments. An antiserum raised against the RSD of human NFATx1 (α-DS) specifically immunoprecipitated a band of 137 kDa from lysates derived from NFATx1-transfected cells (Fig. 4A, lanes 1 and 2). Western analyses confirmed that the 137-kDa band corresponded to NFATx1 (19). When lysates from cells transfected with all three expression plasmids pME-NFATx1, pBJ5-CNA, and pBJ5-CNB were used, the antiserum α-DS coimmunoprecipitated NFATx1 with both CNA (~57 kDa) and CNB (~18 kDa) (Fig. 4A, lane 3). Conversely, an antiserum raised against murine CNB (α-CNB) was able to coimmunoprecipitate CNB with CNA and NFATx1 (Fig. 4B, lanes 1 to 3). These results indicated that NFATx1, like NFAT1, closely associated with calcineurin.

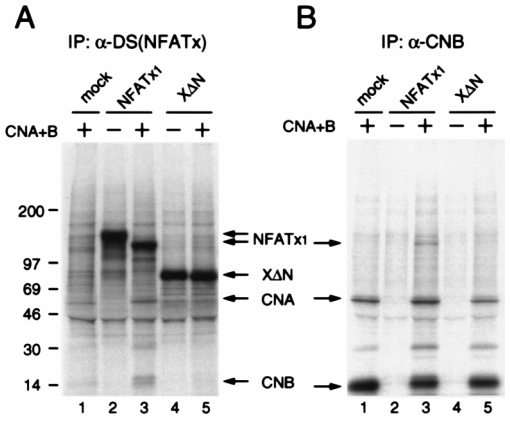

FIG. 4. Calcineurin associates with the N-terminal domain of NFATx1. Immunoprecipitations (IP) using antisera raised against NFATx (A) or CNB (B) were performed on ^{35}S-labeled cell extracts from transfected-293T cells. Transfections were carried out with 20 μg of expression plasmids for NFATx1 or XΔN and/or 5 μg each of expression plasmids for CNA and CNB. Where needed, vector pME18S was added to obtain 30 μg of total transfected plasmid amounts. Immunoprecipitated proteins were resolved on SDS–8 to 16% polyacrylamide gels and visualized by autoradiography on X-ray film (BIOMAX; Kodak). Arrows indicate positions for NFATx1, XΔN, CNA, and CNB as determined by Western blot analyses (19). Size markers for panel A are shown in kilodaltons on the left.

Two other bands of ~29 and ~19 kDa of unknown identity also coimmunoprecipitated with NFATx1 (Fig. 4A, lane 3). These bands were also present in lysates from CNA- and CNB-transfected cells when immunoprecipitated with α-CNB antiserum (Fig. 4B, lane 1), suggesting that these proteins coimmunoprecipitated with NFATx1 through their association with calcineurin. Their function in the multimeric NFATx1-calcineurin complex awaits further characterization. It is also possible that these bands represent degradation products or modified peptides deriving from pBJ5-CNA and pBJ5-CNB. However, they were not detected by Western blotting experiments with various anticalcineurin antisera (19).

We next checked whether XΔN, which could drive transcription without calcineurin activity, could also bind calcineurin. In sharp contrast to NFATx1, XΔN failed to be coimmunoprecipitated with calcineurin in assays using either α-DS or α-CNB antiserum (Fig. 4). These results indicate that calcineurin bound NFATx1 via its amino-terminus domain and are consistent with results of transfection experiments that suggested the N-terminal domain of NFATx1 was a target for calcineurin action.

Importantly, the NFATx1 interaction with calcineurin was accompanied by a mobility shift of NFATx1 in SDS-PAGE, indicating a change in molecular size from 137 to 120 kDa (Fig. 4, lanes 2 and 3). Once again, the mobility shift was absent when XΔN was used instead of NFATx1, reinforcing the idea that the shift was caused by calcineurin action on the N-terminal domain. Thus, these results strongly support the idea that the mobility shift is dependent on the dephosphorylation of residues present in the N-terminal domain. Calcineurin, a phosphoserine/threonine phosphatase, would have several potential target residues since serine is the most abundant amino acid in the N-terminal domain (67 of 418 residues).

Taken together, the foregoing results suggest that the dependency of NFATx1 activity on calcium signaling is mediated by an inhibitory sequence located in its N terminus. Hereafter, we will refer to this sequence conferring calcineurin-regulated inhibition as the CRI sequence. The results show that calcineurin binds to the N terminus of NFATx1 and deactivates the inhibitory activity of the CRI sequence, allowing NFATx1 to become transcriptionally active.

Mapping of the CRI sequence in NFATx1. We next tried to map the residues responsible for the CRI activity. For this purpose, we made a series of plasmids containing further deletions within the N-terminal domain of NFATx1 and used the PMA-only transactivation activity in Jurkat cells as an assay (Fig. 5).

First, the deletion in XΔN was divided into XΔXX and XΔXM (Fig. 5A), the results clearly indicating that the CRI sequence was present in XΔXM (Fig. 5B). Next, the deletion in XΔXM was divided into XΔXB and XΔBM (Fig. 5A). Interestingly, transfection of pME-XΔXB resulted in even higher PMA-induced activity. On the other hand, XΔBM was unable to induce any transactivation by PM alone (Fig. 5B).

XΔXB contains a deletion that included the three previously recognized SP boxes (21) in addition to 60 residues preceding them. Thus, the deletion in XΔXB was divided into XΔBB and XΔGT (Fig. 5A). Unmistakably, deletion of the 60 amino acids

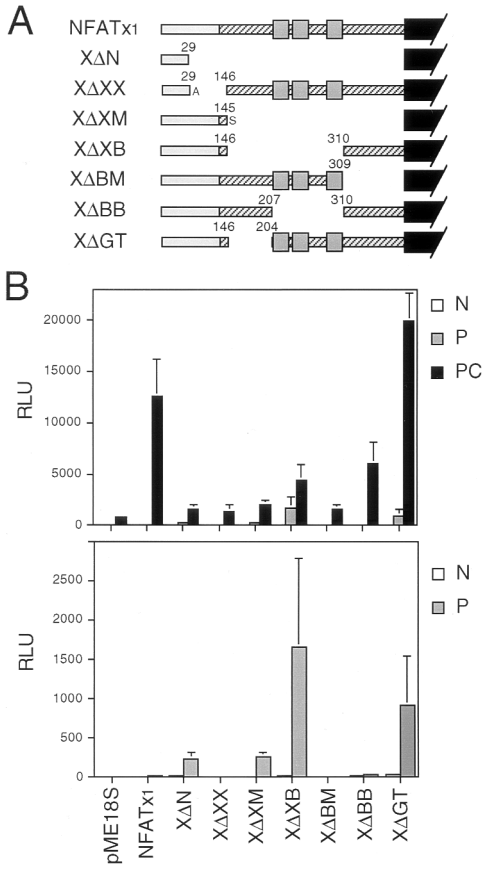

FIG. 5. Mapping of the inhibitory region in NFATx1. (A) Schematic diagram of in-frame deletions within the N-terminal domain of NFATx1. Only the N-terminal domains, with numbers indicating the position of residues remaining in the deletions, are shown. The extra alanine and serine residues shown in XΔXX and XΔXM, respectively, were inserted by the junctions used for their plasmid constructions. (B) Jurkat cells were transfected with 15 μg of the indicated expression plasmids along with pNFAT72Luc (3 μg) and pCMV-SEAP (3 μg). Luciferase activity was measured and normalized as for Fig. 3. The data are averages of three independent experiments. The lower panel is the same as the upper panel but shows only the values for nonstimulated cells and PMA-only-stimulated cells. Abbreviations are as defined in the legend to Fig. 3.

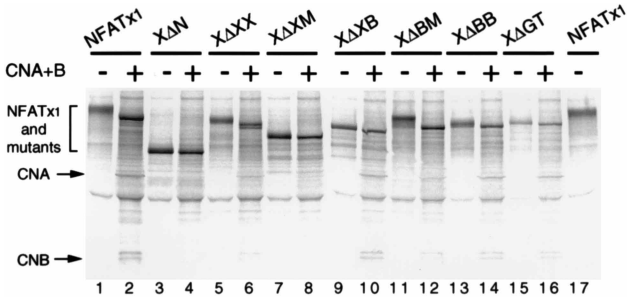

FIG. 6. Multiple docking sites for calcineurin in the N-terminal domain of NFATx1. Immunoprecipitation experiments were carried out as for Fig. 4 except that 293T cells were separately transfected with either 20 μg of the corresponding NFATx1 expression plasmid or 15 μg each of expression plasmids for CNA and CNB. Extracts were combined as indicated for 5 min on ice prior to addition the anti-NFATx1 antisera. Arrows indicate the positions for CNA and CNB.

preceding the SP boxes in XΔGT resulted in PMA-induced activity, while deletion of the SP boxes in XΔBB did not (Fig. 5B). These results indicate that deletion of at least 60 residues was sufficient for inactivating the inhibitory activity conferred by the CRI sequence.

Comparison of the 60 residues deleted in XΔGT to analogous sequences of other NFAT proteins shows that this sequence has been only loosely conserved (Fig. 1B). The first 40 residues are weakly conserved in all NFAT proteins centered around two motifs: YR(E,D) and SSXSSXSXXS(D,E). In NFAT3, an additional octapeptide has been inserted between the two motifs. These 40 residues closely corresponded to the A box, which was reported by Hoey et al. (10) to be conserved between NFATc and NFATx. The 20 amino acids at the carboxy end of the 60-residue peptide are absent or partially absent in NFAT1 and NFATc but are nicely conserved between NFATx1 and NFAT3 (Fig. 1B). It will be interesting to see whether these sequences play similar roles in their respective NFAT contexts.

Strikingly, the deletion in XΔGT caused no adverse effect on transactivation when cells were induced by the combination of PMA and A23187 (Fig. 5B), indicating that CRI function could be separated from the effects on transactivation seen with XΔN. Supporting this idea is the fact that the converse was observed with XΔBM and XΔBB, which appeared to have little effect on CRI activity but affected PMA-A23187-induced transcriptional activity.

It should be noted that conclusions drawn from the XΔXX construct are complicated because all transactivation activity was abolished. Other constructs showed at least modest induction over endogenous NFAT activity (Fig. 5). The mutant XΔXX protein could be detected and was therefore being expressed (19). However, it is possible that the XΔXX structure, and therefore its function, was defective and thus compromised much of its transactivation activity.

Multiple docking sites for calcineurin in the N terminus of NFATx1. We next performed immunoprecipitation experiments with the N-terminus deletions to investigate whether sequences affecting CRI function correlated with calcineurin binding (Fig. 6). To ensure that the amounts of calcineurin in lysates were identical from experiment to experiment, we slightly modified the experimental protocol whereby equal amounts of the lysate from 293T cells transfected with pBJ5-CNA and pBJ5-CNB were mixed with lysates from 293T cells that had been separately transfected with pME-NFATx1 or its derivatives. The results with NFATx1 and XΔN (Fig. 6, lanes 1 to 4) were essentially identical to results depicted in Fig. 4A.

Remarkably, XΔGT coimmunoprecipitated with calcineurin (Fig. 6, lane 16). This meant that calcineurin binding did not necessarily correlate with CRI function. In other words, calcineurin binding was not sufficient to inactivate the inhibitory activity. In fact, apart from XΔN and XΔXM, the deletion mutants were able to associate with calcineurin (Fig. 6). A simple interpretation of these results, as far as calcineurin binding is concerned, is that calcineurin was capable of binding NFATx1 at different sites within the N-terminal domain of NFATx1; only when all the docking sites were deleted was calcineurin binding lost. This finding again is supported by the observation that serine is the most abundant amino acid throughout this region, possibly providing multiple substrates and pseudosubstrates for calcineurin. It is not known whether more than one calcineurin molecule binds NFATx1 at any one time.

Significantly, even though calcineurin bound to several of the mutant NFATx1 proteins, the calcineurin-induced shift of NFATx1 mobility in SDS-PAGE was not observed in all NFATx1 mutants (Fig. 6). Specifically, a clear calcineurin-induced shift was observed in full-length NFATx1, XΔXX, and

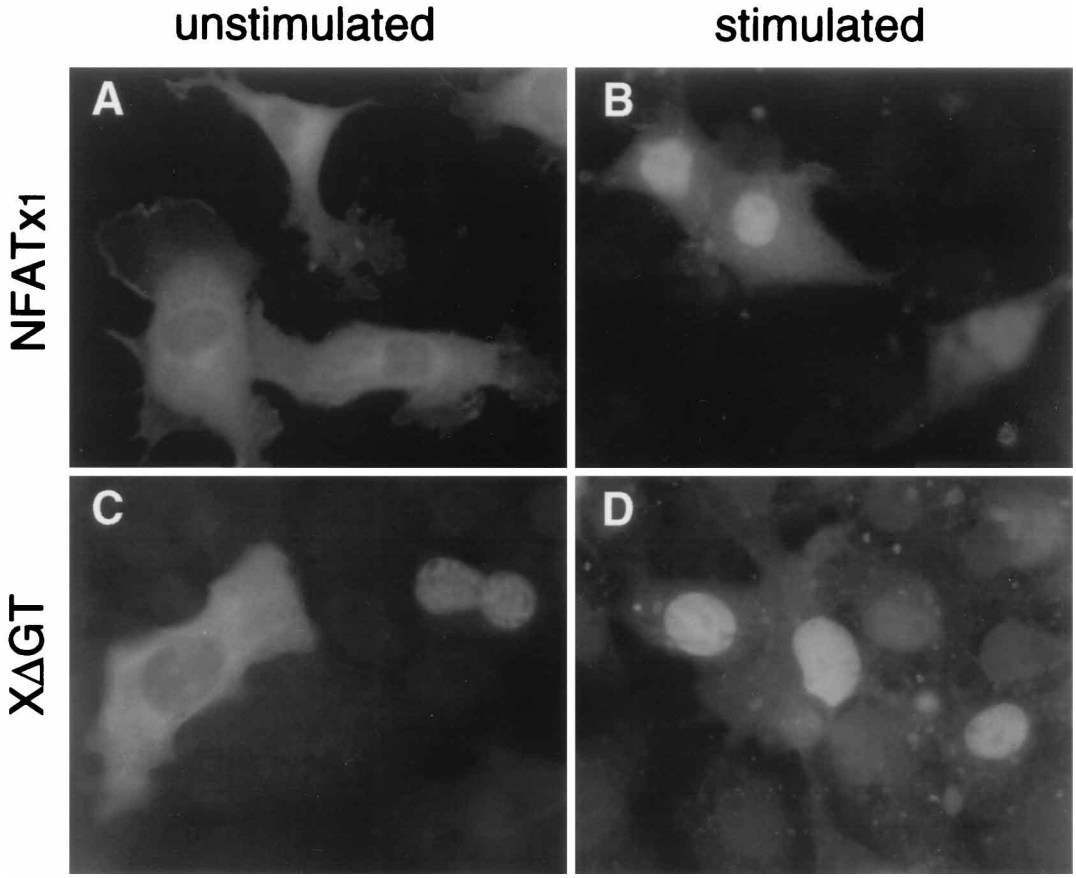

FIG. 7. Intracellular localization of recombinant NFATx1 and XΔGT in COS-7 cells. Cells were transfected with expression plasmids for NFATx1 (A and B) and XΔGT (C and D) along with expression plasmids for CNA and CNB. Transfected cells were either left unstimulated (A and C) or stimulated for 30 min with the calcium ionophore A23187 (0.5 μM) (B and D). Recombinant proteins were visualized by immunofluorescence staining with affinity-purified polyclonal antibody α-DS, which recognizes the RSD of NFATx1.

XΔBM (Fig. 6, lanes 1, 2, 5, 6, 11, and 12); on the other hand, the calcineurin-induced shift was reduced or absent in XΔN, XΔXM, XΔXB, XΔBB, and XΔGT (Fig. 6, lanes 3, 4, 7, 8, 9, 10, 13, 14, 15, and 16). Except for XΔBB, the calcineurin-induced shift correlated with CRI activity seen in Fig. 5. That is, when sequences affecting CRI function were deleted, the calcineurin-induced shift in SDS-PAGE was reduced. These results suggest that certain residues were susceptible to calcineurin phosphatase action, as could be observed by mobility shifts in SDS-PAGE, and that deletion of these residues lead to calcium-independent activation. Collectively, the results indicate that calcineurin binds to the N terminus of NFATx1 at multiple sites and dephosphorylates residues in the CRI sequence, deactivating its inhibitory activity.

Intracellular localization of NFATx1 and XΔGT. To obtain further insight into the mechanism of the CRI activity, we then decided to examine the intracellular localization of NFATx1 and XΔGT in transfected COS-7 cells. Recently, we showed by immunostaining using affinity-purified α-DS antibodies that murine NFATx1 introduced into COS-7 cells localized predominantly to the cytoplasm (14). We also showed that endogenous calcineurin levels in our COS-7 cells were insufficient to drive efficient nuclear translocation of transfected murine NFATx1; only when CNA and CNB were also overexpressed by cotransfection did most of the murine NFATx1 translocate into the nucleus in response to calcium ionophore (A23187) stimulation (14). We then transfected COS-7 cells with pME-NFATx1 or pME-XΔGT along with expression plasmids for CNA and CNB and immunostained them by using α-DS antibodies (Fig. 7). The results showed that, similar to murine NFATx1, essentially all human NFATx1 (>95%) localized to the cytoplasm of COS-7 cells (Fig. 7). Moreover, induction of calcium mobilization by A23187 treatments resulted in nuclear localization of NFATx1 in about 85% of the NFATx1-expressing cells, showing that NFATx1 nuclear localization was dependent on calcium signaling.

On the other hand, XΔGT localized to the nucleus in 70 to 80% of nonstimulated COS-7 cells that expressed XΔGT (Fig. 7). A23187 treatments resulted in an increase of XΔGT nuclear localization to over 90% of XΔGT-expressing cells. These results demonstrate that an activity that normally retains NFATx1 in the cytoplasm was disrupted by the deletion in XΔGT, thus providing one mechanism for the inhibitory activity conferred by the CRI sequence in NFATx1.

DISCUSSION

Based on sequence comparisons, we divided NFATx1 into three domains. Our results confirmed that the RSD, located in the middle of NFATx, was responsible for DNA binding activity and for interactions with AP-1 polypeptides (Fig. 2C). This finding is consistent with results of assays using the DNA-binding domain of the NF-κB/Rel protein family (3) and, more

specifically, with analogous results of assays using the NFAT1 RSD (12, 22).

As for sequences in both the amino terminus and the carboxy terminus of NFATx, our results indicated that they play important roles in the regulation and transactivation function of NFATx1 (Fig. 3). In fact, recently we have identified a 15-amino-acid motif close to the carboxy end of NFATx1 that is responsible for transactivation activity in NFATx1 (11). This finding further supports the idea that a main role for the C terminus is to mediate transcriptional induction via its transactivation sequences. The presence of a strong transactivation domain in the C terminus of NFAT1C, a splice variant of NFAT1, has also been recently reported (17).

Interestingly, deletion of the amino-terminal domain also revealed that this region contained an inhibitory sequence that was regulated by calcium signaling (Fig. 3). We refer to this sequence as the CRI sequence and its negative activity as CRI activity. Thus, we showed that the CRI activity, which would be normally inactivated by calcium mobilization, could also be removed by specific deletions within the N terminus. In the absence of CRI activity, as in an NFATx1 lacking the N terminus (XΔN), transcriptional activation did not require the calcium signaling pathway, and this transactivation was insensitive to the action of the calcineurin inhibitor CsA (Fig. 3).

Recent work on NFAT1 regulation has established that upon stimulation, calcineurin binds to the amino terminus region of NFAT1, which is then dephosphorylated and subsequently translocated to the nucleus (18, 30, 32). Our present work involving the similarly regulated NFATx1 extends these observations. We found not only that calcineurin bound the amino terminus of NFATx1 but that it did so by using multiple docking sites (Fig. 6). Moreover, we also mapped the sequences (positions 146 to 310 in Fig. 1B) containing target residues of calcineurin activity, as shown by the reduced calcineurin-induced mobility shift of XΔGT and XΔBB mutants (Fig. 6).

Our results also complement two other recent reports. Shibasaki et al. (33) showed that calcineurin bound the N terminus of NFAT4/x and was translocated into the nucleus in conjunction with NFAT4/x. Our results are consistent with theirs and further show that calcineurin association to NFATx1 alone is insufficient to transmit the calcium-regulated signal, for it is the calcineurin-induced size shifts (dephosphorylations) that appear to correlate with CRI function. For example, of the several mutants that were able to bind calcineurin, only those with reduced calcineurin-induced shifts XΔXB and XΔGT bypassed calcium signaling (Fig. 5 and 6). XΔBB appears to be an exception and will be discussed below.

Likewise, Luo et al. (17) showed that deletion of all of the N-terminal domain of NFAT1C, a splice variant of NFAT1, resulted in transactivation induced by PMA alone. They further showed, using fusions to the GAL4 DNA-binding domain, that the N-terminus sequence could be subdivided into two functional domains: a strong transactivation domain, contained in the first 100 residues; and a region potently inhibiting transactivation, contained in the NHR of ~300 residues. Again, our results are consistent. We show a similar inhibitory sequence in the N terminus of NFATx1. Moreover, we have mapped this region to 60 residues just preceding the SP boxes (Fig. 1B), showing that when it is deleted, the calcium-signaling dependence is partially bypassed (Fig. 5B).

The mechanism for the calcium-regulated inhibition is complicated by the fact that three possible steps may be affected: nuclear translocation, DNA binding, and transactivation. It is possible the CRI function affects one, two, or all three of these activities.

The foregoing caveat notwithstanding, it is clear that nuclear translocation must occur before the other two activities become relevant. Furthermore, it has been shown that NFATx translocates into the nucleus in a calcineurin-dependent manner (14, 33). Our results here clearly showed that CRI, at minimum, regulates NFATx1 nuclear translocation. Unlike NFATx1, the deletion mutant XΔGT containing a disrupted CRI function was able to localize to the nucleus independently of calcium signaling in COS-7 cells (Fig. 7).

There are two main nonexclusive models for the mechanism for the regulation of NFATx1 translocation. One model is simply that the 60 residues adjacent to the SP boxes would impart retention in the cytoplasm to NFATx1 via specific protein-protein interactions. The phosphatase activity of calcineurin on some of the residues would then be required for the subsequent NFATx1 release. In this respect, it will be interesting to examine the function of the YR(E,D) and SSXSSXSXXS(D,E) motifs present in the 60 residues (Fig. 1B).

The concept for the alternative model is also facilitated by considering that it is likely that the CRI sequence constitutes a structural module, or part of it, that retains NFATx1 in the cytosol. From sequence comparisons, it is pertinent to assume that the module could correlate to the NHR, which is conserved in all NFAT proteins (Fig. 1). That is, CRI activity might require a span of ~300 residues instead of a few residues. In this model, nuclear localization signals (NLSs) are being masked by amino acids in the CRI sequence. As calcium is mobilized, calcineurin is activated and would bind to the amino terminus of NFATx1. Activated calcineurin would then dephosphorylate residues present in the CRI sequence, causing a structural change that would lead to the unmasking of NLSs. NFATx1 would then go into the nucleus and activate gene expression in conjunction with PMA-induced AP-1. Similar versions of this model have been recently proposed (4, 18, 33).

Indeed, detailed examination of the aligned NFAT sequences revealed basic conserved motifs flanking the SP box closest to the Rel domain (Fig. 1) (16) that may function as NLSs. In fact, one of these motifs, the RXXSPXXKRRXS motif, was recently shown to form part of a NLS by Luo et al. (18). Their amino acid substitutions of the KRR residues in this motif for AAA residues resulted in an NFAT1 unable to translocate into the nucleus upon stimulation. The function of the other basic motif remains unknown.

In this scenario, the NLSs would be masked by the surrounding acidic motifs, e.g., SP boxes. Deletion of the YR(E,D) and SSXSSXSXXS(D,E) motifs, preceding the SP boxes, in XΔGT would cause some unmasking of the NLSs, leading to its translocation to the nucleus (Fig. 7). In the cases where the basic motifs in the N-terminal domain have been deleted (e.g., XΔN, XΔXM, and XΔXB), yet another putative NLS in the RSD (3, 10, 21) might be responsible for their nuclear translocation. It should be noted however, that the nuclear localization function of this alternative NLS appears to be weak. Immunostaining experiments showed that although XΔXB could be found in the nucleus without calcium signaling, this occurred in only about 10% of the transfected COS cells (as opposed to 70 to 80% of cells that were transfected with XΔGT) (19).

Unexpectedly, deletion of the SP boxes in XΔBB (Fig. 5), which also deleted a putative NLS, did not result in transactivation stimulated by PMA alone. Conceivably, this deletion should disrupt the module responsible for CRI function. Thus, this appears to indicate that the YR(E,D) and SSXSSX SXXS(D,E) motifs in the 60 residues preceding the SP boxes have a potent intrinsic inhibitory activity as proposed in the

first model. It is then possible that the models mentioned above are both operating. That is, the CRI activity could be composed of sequences that retain NFATx1 in the cytoplasm and sequences that mask intrinsic NLSs. Future experiments should help us understand the details of this apparently complex regulation of NFATx1 activity.

In addition to nuclear translocation, it has been reported that calcineurin also regulates DNA binding of NFAT1 (26). At present, we do not know whether the CRI sequence affects NFATx1 DNA binding. We also do not know whether the mapped 60 residues can mask transactivation domains in a manner that would be calcium-calcineurin regulated, as suggested in NFAT1 regulation (17).

An interesting observation regarding XΔGT is that the PMA-A23187 transactivation activity was separable from CRI function (Fig. 5). This finding suggested that transactivation and CRI regulation may work independently. However, it was also observed that PMA-alone induction of XΔGT did not recover all activity (Fig. 5). One reason for the incomplete recovery could be that calcium signaling is needed for additional pathways required for NFAT-dependent transcription. This could be within NFATx1. That is, deletion in XΔGT allowed only partial unmasking of putative NLSs, and further calcineurin action on the remaining residues was needed to allow complete NLS unmasking. Another possibility is that calcium signaling could be required independently of NFATx1. For example, calcineurin has been shown to affect Jun kinase activity (34) and AP-1 activity (29). Fully activated AP-1 would then join XΔGT, resulting in maximal transactivation.

Again, from comparison of XΔGT with XΔXB, it is apparent that the SP boxes affect PMA-A23187-induced transactivation (Fig. 5). Likewise, deletions other than XΔGT affect PMA-A23187 transactivation. It is possible that the deletions caused structural defects that would affect nuclear translocation and/or DNA binding. Alternatively, bona fide transactivation domains are present in the amino terminus of NFATx1, and their deletion would affect transactivation. Future experiments will tell us whether the downregulation was due to direct effects on transactivation.

The discrepancy between the deduced and apparent sizes of NFATx1 in SDS-polyacrylamide gels indicated that its amino terminus was modified. The activities causing these modifications were present and constitutively activated in Jurkat, COS-7, and 293T cells (19). Further deletions within the amino terminus indicated that in fact there were multiple modifications, since no particular deletion could account for all the mobility shift. That is, a gradual reduction of molecular size discrepancy was observed as different regions were deleted (Fig. 6) (19). The shift-down caused by calcineurin accounted for three-fourths of the molecular size discrepancy. Thus, it appears that other modifications, not regulated by calcineurin, exist to account for the other fourth of the discrepancy.

The generality of the CRI regulation in NFAT proteins is implied by the conservation of N-terminal motifs in the NFAT proteins, since they were presumably maintained through evolution for similar regulatory functions. This might explain why most, if not all, NFAT proteins activities are regulated by calcium signaling and inhibited by CsA (10, 16). Nevertheless, differences may also be expected since there are considerable dissimilarities and gaps within motifs in the different NFAT proteins (Fig. 1B) (16). Similar deletions in other NFAT proteins, coupled to chimera constructions, should shed some light on their similarities and differences.

Finally, our coimmunoprecipitation experiments showed that calcineurin physically associated with its substrate NFATx1 even after it had been already dephosphorylated. This finding appears counterintuitive, but we believe that it is a necessary step to offset the activity of a potent constitutive NFAT kinase (33). Negative regulation by a constitutive kinase may be used to provide a rapid repression of NFAT action once the inducer is removed. Consistent with this idea is the fact that the association is also seen in the nucleus. We found that when calcineurin was cotransfected into COS cells with NFATx1, both proteins colocalized in the nucleus after stimulation of the calcium signaling pathway. In the absence of NFATx1, on the other hand, calcineurin localized throughout the whole cell regardless of the stimulation status of the cells (19).

Another significant outcome for the interplay of a kinase and a phosphatase on multiple residues in NFAT is that it could be used as a mechanism to ensure that NFAT responds only upon sustained calcium mobilization. Recently, T-cell responses were shown to depend on the activation of a threshold number of T-cell receptors (35). This threshold was correlated with the duration of calcium mobilization. It is possible that NFAT proteins uphold this type of regulation by responding only when a certain threshold level of mobilized calcium is sustained to allow activated calcineurin to bind and inactivate CRI function. In this case, controlling the amount and duration of the calcium that is mobilized would determine whether NFAT proteins carry on with their transactivation activities.

ACKNOWLEDGMENTS

We are grateful to Lisako Tsuruta for providing pNFAT72Luc, Debra Ligget for oligonucleotide synthesis, Allison Helms for DNA sequencing, and Emma Lees for advice on immunoprecipitation experiments. We thank J. Fernando Bazan, Anjana Rao, and Patrick Hogan for helpful discussions and Dovie Wylie for reading the manuscript.

DNAX Research Institute of Molecular and Cellular Biology is supported by Schering-Plough Co.

REFERENCES

1. **Arai, K. I., F. Lee, A. Miyajima, S. Miyatake, N. Arai, and T. Yokota.** 1990. Cytokines: coordinators of immune and inflammatory responses. Annu. Rev. Biochem. **59:**783–836.
2. **Ausubel, F. M., R. Brent, R. E. Kingston, D. D. Moore, J. G. Seidman, J. A. Smith, and K. Struhl (ed.).** 1987. Current protocols in molecular biology. Greene Publishing Associates and Wiley-Interscience, New York, N.Y.
3. **Baeuerle, P. A., and T. Henkel.** 1994. Function and activation of NF-kappa B in the immune system. Annu. Rev. Immunol. **12:**141–179.
4. **Chytil, M., and G. L. Verdine.** 1996. The rel family of eukaryotic transcription factors. Curr. Opin. Struct. Biol. **6:**91–100.
5. **Clipstone, N. A., and G. R. Crabtree.** 1992. Identification of calcineurin as a key signalling enzyme in T-lymphocyte activation. Nature **357:**695–697.
6. **Crabtree, G. R., and N. A. Clipstone.** 1994. Signal transmission between the plasma membrane and nucleus of T lymphocytes. Annu. Rev. Biochem. **63:**1045–1083.
7. **DuBridge, R. B., P. Tang, H. C. Hsia, P. M. Leong, J. H. Miller, and M. P. Calos.** 1987. Analysis of mutation in human cells by using an Epstein-Barr virus shuttle system. Mol. Cell. Biol. **7:**379–387.
8. **Harlow, E., B. J. Franza, and C. Schley.** 1985. Monoclonal antibodies specific for adenovirus early region 1A proteins: extensive heterogeneity in early region 1A products. J. Virol. **55:**533–546.
9. **Ho, S. N., D. J. Thomas, L. A. Timmerman, X. Li, U. Francke, and G. R. Crabtree.** 1995. NFATc3, a lymphoid-specific NFATc family member that is calcium-regulated and exhibits distinct DNA binding specificity. J. Biol. Chem. **270:**19898–19907.
10. **Hoey, T., Y. L. Sun, K. Williamson, and X. Xu.** 1995. Isolation of two new members of the NF-AT gene family and functional characterization of the NF-AT proteins. Immunity **2:**461–472.
11. **Imamura, R., E. S. Masuda, Y. Naito, S. Imai, T. Fujino, T. Takano, K. Arai, and N. Arai.** Submitted for publication.
12. **Jain, J., E. Burgeon, T. M. Badalian, P. G. Hogan, and A. Rao.** 1995. A similar DNA-binding motif in NFAT family proteins and the Rel homology region. J. Biol. Chem. **270:**4138–4145.
13. **Jain, J., C. Loh, and A. Rao.** 1995. Transcriptional regulation of the IL-2 gene. Curr. Opin. Immunol. **7:**333–342.
14. **Liu, J., N. Koyano-Nakagawa, Y. Amasaki, F. Saito-Ohara, T. Ikeuchi, S.**

Imai, T. Takano, N. Arai, T. Yokota, and K. Arai. 1997. Calcineurin dependent nuclear translocation of a murine transcription factor NFATx: molecular cloning and functional characterization. Mol. Biol. Cell **8:**157–170.
15. **Loh, C., K. T.-Y. Shaw, J. Carew, J. P. B. Viola, C. Luo, B. A. Perrino, and A. Rao.** 1996. Calcineurin binds the transcription factor NFAT1 and reversibly regulates its activity. J. Biol. Chem. **271:**10884–10891.
16. **Luo, C., E. Burgeon, J. A. Carew, P. G. McCaffrey, T. M. Badalian, W. S. Lane, P. G. Hogan, and A. Rao.** 1996. Recombinant NFAT1 (NFATp) is regulated by calcineurin in T cells and mediates transcription of several cytokine genes. Mol. Cell. Biol. **16:**3955–3966.
17. **Luo, C., E. Burgeon, and A. Rao.** 1996. Mechanisms of transactivation by nuclear factor of activated T cells-1. J. Exp. Med. **184:**141–147.
18. **Luo, C., K. T.-Y. Shaw, A. Raghavan, J. Aramburu, F. Garcia-Cozar, B. A. Perrino, P. G. Hogan, and A. Rao.** 1996. Interaction of calcineurin with a domain of the transcription factor NFAT1 that controls nuclear import. Proc. Natl. Acad. Sci. USA **93:**8907–8912.
19. **Masuda, E. S., J. Liu, and R. Imamura.** Unpublished data.
20. **Masuda, E. S., Y. Naito, K. Arai, and N. Arai.** 1993. Expression of lymphokine genes in T cells. Immunologist **1:**198–203.
21. **Masuda, E. S., Y. Naito, H. Tokumitsu, D. Campbell, F. Saito, C. Hannum, K. Arai, and N. Arai.** 1995. NFATx, a novel member of the nuclear factor of activated T cells family that is expressed predominantly in the thymus. Mol. Cell. Biol. **15:**2697–2706.
22. **McCaffrey, P. G., C. Luo, T. K. Kerppola, J. Jain, T. M. Badalian, A. M. Ho, E. Burgeon, W. S. Lane, J. N. Lambert, T. Curran, et al.** 1993. Isolation of the cyclosporin-sensitive T cell transcription factor NFATp. Science **262:** 750–754.
23. **Mosmann, T. R., and R. L. Coffman.** 1989. TH1 and TH2 cells: different patterns of lymphokine secretion lead to different functional properties. Annu. Rev. Immunol. **7:**145–173.
24. **Northrop, J. P., S. N. Ho, L. Chen, D. J. Thomas, L. A. Timmerman, G. P. Nolan, A. Admon, and G. R. Crabtree.** 1994. NF-AT components define a family of transcription factors targeted in T-cell activation. Nature **369:**497–502.
25. **O'Garra, A., and K. Murphy.** 1996. Role of cytokines in development of Th1 and Th2 cells. Chem. Immunol. **63:**1–13.
26. **Park, J., N. R. Yaseen, P. G. Hogan, A. Rao, and S. Sharma.** 1995. Phosphorylation of the transcription factor NFATp inhibits its DNA binding activity in cyclosporin A-treated human B and T cells. J. Biol. Chem. **270:** 20653–20659.
27. **Rao, A.** 1994. NF-ATp: a transcription factor required for the co-ordinate induction of several cytokine genes. Immunol. Today **15:**274–281.
28. **Rao, A.** 1991. Signaling mechanisms in T cells. Crit. Rev. Immunol. **10:**495–519.
29. **Rincon, M., and R. A. Flavell.** 1994. AP-1 transcriptional activity requires both T-cell receptor-mediated and co-stimulatory signals in primary T lymphocytes. EMBO J. **13:**4370–4381.
30. **Ruff, V. A., and K. L. Leach.** 1995. Direct demonstration of NFAT dephosphorylation and nuclear localization in activated HT-2 cells using a specific NFAT polyclonal antibody. J. Biol. Chem. **270:**22602–22607.
31. **Shaw, J. P., P. J. Utz, D. B. Durand, J. J. Toole, E. A. Emmel, and G. R. Crabtree.** 1988. Identification of a putative regulator of early T cell activation genes. Science **241:**202–205.
32. **Shaw, K. T., A. M. Ho, A. Raghavan, J. Kim, J. Jain, J. Park, S. Sharma, A. Rao, and P. G. Hogan.** 1995. Immunosupressive drugs prevent a rapid dephosphorylation of transcription factor NFAT1 in stimulated immune cells. Proc. Natl. Acad. Sci. USA **92:**11205–11209.
33. **Shibasaki, F., E. R. Price, D. Milan, and F. McKeon.** 1996. Role of kinases and the phosphatase calcineurin in the nuclear shuttling of the transcription factor NF-AT4. Nature **382:**370–373.
34. **Su, B., E. Jacinto, M. Hibi, T. Kallunki, M. Karin, and N. Y. Ben.** 1994. JNK is involved in signal integration during costimulation of T lymphocytes. Cell **77:**727–736.
35. **Viola, A., and A. Lanzavecchia.** 1996. T cell activation determined by T cell receptor number and tunable thresholds. Science **273:**104–106.
36. **Watanabe, M., M. Muramatsu, H. Hirai, T. Suzuki, J. Fujisawa, M. Yoshida, K. Arai, and N. Arai.** 1993. HTLV-I encoded Tax in association with NF-kappa B precursor p105 enhances nuclear localization of NF-kappa B p50 and p65 in transfected cells. Oncogene **8:**2949–2958.
37. **Wesselborg, S., D. A. Fruman, J. K. Sagoo, B. E. Bierer, and S. J. Burakoff.** 1996. Identification of a physical interaction between calcineurin and nuclear factor of activated T cells (NFATp). J. Biol. Chem. **271:**1274–1277.